Journal of
Nanoscience and Nanotechnology
Vol. 6, 337–344, 2006

Polyethylene Organo-Clay Nanocomposites: The Role of the Interface Chemistry on the Extent of Clay Intercalation/Exfoliation

Michaël Mainil,[1,2] Michaël Alexandre,[1,2] Fabien Monteverde,[2] and Philippe Dubois[1,2,*]

[1] *Laboratory of Polymeric and Composite Materials, University of Mons-Hainaut, Place du Parc 20, 7000 Mons, Belgium*
[2] *Materia Nova Research Center, Avenue N. Copernic 1, 7000 Mons, Belgium*

High density polyethylene (HDPE)/clay nanocomposites have been prepared using three different functionalized polyethylene compatibilizers: an ethylene/vinyl acetate copolymer, a polyethylene grafted with maleic anhydride functions and a (styrene-b-ethylene/butylene-b-styrene) block copolymer. The nanocomposites were prepared via two different routes: (1) the dispersion in HDPE of a masterbatch prepared from the compatibilizer and the clay or (2) the direct melt blending of the three components. For each compatibilizer, essentially intercalated nanocomposites were formed as determined by X-ray diffraction and transmission electron microscopy. With the ethylene/vinyl acetate copolymer, a significant delamination of the intercalated clay in thin stacks was observed. This dispersion of thin intercalated stacks within the polymer matrix allowed increasing significantly the stiffness and the flame resistance of the nanocomposite. A positive effect of shear rate and blending time has also been put into evidence, especially for the process based on the masterbatch preparation, improving both the formation of thin stacks of intercalated clay and the mechanical properties and the flame resistance of the formed nanocomposites.

Keywords: Nanocomposite, Polyethylene, Montmorillonite, Intercalation, Layered Silicate.

1. INTRODUCTION

Polymer/layered silicate nanocomposites[1–3] represent innovative materials that have proven to be very attractive for food, construction, and transportation industries[4] owing to their improved thermo-mechanical,[5,6] fluids barrier[7,8] and flame-retardant properties.[9] This new kind of material is usually composed of a few weight percents of aluminosilicate nanolayers well dispersed in a polymer matrix. These nanolayers (1 nm thick and hundreds nanometers in diameter) originate from stacked natural or organomodified clays such as montmorillonite. Once isolated and dispersed, these nanolayers provide high contact surface (more than 700 m^2/g) with the polymer matrix and can reinforce the latter. Nevertheless, such an ideal dispersion requires the polymer and the clay to be chemically compatible. This condition can be relatively easily fulfilled for polymers including polar (functional) groups such as poly(amide)s,[10–13] polystyrene[14–16] or poly(ester)s.[17] Indeed, when the polymer—(organomodified) clay interactions are more favorable than polymer–polymer or clay–clay interactions, there is a spontaneous diffusion of the chains from the bulk into the galleries, which forces the spacings between clay nanolayers to increase: this is intercalation. When the interactions are highly favorable and if the melt blend is submitted to efficient kneading conditions, the intercalated chains may cause the delamination (exfoliation) of the stacks leading to the dispersion of isolated nanolayers in the whole matrix.

Polyethylene (PE) is one of the most used polymers in the world owing to its extraordinary large panel of thermomechanical properties, ranging from the highly flexible low density and very low density PE (LDPE and VDPE), through the tough and yet flexible high density polyethylene (HDPE) to ultrahigh molecular weight polyethylene (UHMWPE) used to prepare very resistant and stiff PE fibers. During the last decade, several routes have been developed to disperse a few weight percents of aluminosilicate nanolayers into PE (and more particularly HDPE) to prepare high-performance nanocomposites. But in the case of a polar HDPE, the lack of favorable interactions even with lipophilic organoclays[18–20] implies more specific

*Author to whom correspondence should be addressed.

1533-4880/2006/6/337/008 doi:10.1166/jnn.2006.007

preparation techniques. For instance, several studies have focused on the *in-situ* (co)polymerization of ethylene within (organo)clays surface-treated by an adequate coordination catalyst.[21–24] However, direct melt blending seems to remain economically more interesting since it limits cost and time of production and avoids the use of any organic solvent. In order to obtain HDPE-based nanocomposites by melt compounding, it is necessary to enhance interfacial interaction between the filler and the matrix. Commercial PE that has been functionalized with a few wt% of polar groups has shown to be able to exfoliate organoclays under shear. Several publications report on the production of intercalated or delaminated nanocomposites by melt blending copolymers such as ethylene/vinyl acetate copolymers with organoclays.[25–28] Maleic anhydride-grafted PE (MAgPE) has also demonstrated its ability to disperse organoclays,[29–31] but has also been used as a compatibilizer of PE–organoclay mixtures.[32]

This study aims at reporting on the preparation of layered silicate nanocomposites through the association of HDPE and Cloisite® 20A (an organomodified montmorillonite which has shown a propensity to exfoliation in both EVA[26] and MAgPE[29] matrices), which structures are thermodynamically stabilized by commercial functionalized ethylene-based (co)polymers used as compatibilizers. Dennis et al.[33] have shown that the residence time and the kneading force applied in extrusion of polyamide-6/Cloisite® blends can directly affect the extent of exfoliation of aluminosilicate layers: excess or lack of blend efficiency precludes the nanoplatelets to disperse in the matrix. Based on these observations, the HDPE/Cloisite® 20A blends were carried out in an internal chamber, which allows for regulating the kneading force and the blending time. Two compounding processes of HDPE, Cloisite® 20A and various compatibilizers have been investigated: (i) Preparation and redispersion of organoclay pre-intercalated with the compatibilizers ("masterbatch" process). (ii) Direct melt blending of all the components. The morphology of the resulting nanocomposites was determined by X-ray diffraction (XRD) and transmission electron microscopy (TEM). The mechanical and flammability properties were also investigated.

RESEARCH ARTICLE

2. EXPERIMENTAL DETAILS

2.1. Materials

HDPE FINATHENE 6410 (HDPE) with a melt flow index under 2.16 kg at 190 °C (MI_2) of 1.2 g/10 min (M_w = 104200 g/mol and M_n = 22500 g/mol) was kindly supplied by ATOFINA Research Feluy. The studied organoclay, Cloisite® 20A was purchased from Southern Clay Products. It is a montmorillonite that is cation-exchanged with 90 meq/100 g of dimethyl di(hydrogenated tallowalkyl) quaternary ammonium salt (24 wt%). Tallow is composed predominantly of octadecyl chains and smaller amounts of lower homologues: the approximate composition was 65% of C_{18}, 30% of C_{16}, and 5% of C_{14}. The organoclay was used as received. Three kinds of commercial functionalized polyethylene samples were used as compatibilizers for the melt blends: (i) a maleic anhydride-grafted polyethylene (MAgPE), Orevac® 18334 from Arkema, actually a modified linear low density polyethylene (LLDPE) copolymer with a MI_2 of 1 and a melting point at 125 °C (maleic anhydride content: more likely less than 1 mol%, average molecular weights unknown); (ii) an ethylene/vinyl acetate copolymer Escorene® UL00112 from Exxon Mobil, with 12 wt% (or 4.25 mol%) in vinyl acetate (EVA_{12}), a MI_2 of 0.5 g/10 min and a melting point at 93 °C (average molecular weights unknown); (iii) a Kraton® G-1652E from Kraton Polymers, a triblock copolymer based on an hydrogenated polybutadiene (10 wt% ethyl branches, M_n = 37000 g/mol) central block and polystyrene (30 wt%, M_n = 7000 g/mol) lateral blocks. Irganox B215 (from Ciba Geigy) was used as antioxidant in all prepared nanocomposites.

2.2. Melt Blending: General Procedure

The nanocomposites (58 g) incorporating different compositions of organoclay and compatibilizer were prepared by melt compounding at 185 °C using an internal mixing chamber (twin-screw Brabender, Cam blade geometry). The screw speed was set at 75 or 20 rpm in order to regulate the shear force. The formed nanocomposites were immediately placed between two metallic plates covered with Teflon and pressed within an AGILA PE20 device for 7 min at 145 °C under 75 bars. It was then quickly cooled down at the temperature of cold water (ca. 15 °C) using the same device and at the same pressure.

2.2.1. Nanocomposite Preparation via the Masterbatch Process (MP): A Two-Step Process

(i) The pellets of the selected compatibilizer were molten on the rolls of an Agila LW100 two-roll mill (rolls speed:10 m/s, distance between rolls fixed at 1.2 mm and kneading ratio of 100), then the antioxidant (0.3 wt%) and Cloisite® 20A were added and blended for 5 min under low shear to prepare a masterbatch compound containing 30 wt% of clay (wt% given in inorganic part). The recovered material was afterwards kneaded in the Brabender mixer for 7 min (at 75 rpm). (ii) The HDPE matrix was melted in the Brabender, added with the previously prepared and finely fragmented masterbatch (i), then the molten compound was kneaded for 7 min or 30 min (at 75 rpm).

2.2.2. Nanocomposite Preparation by Direct Melt Blend Process (DP): A One-Step Process

HDPE pellets were molten in the internal chamber in the presence of 0.3 wt% Irganox B215. Cloisite® 20A and

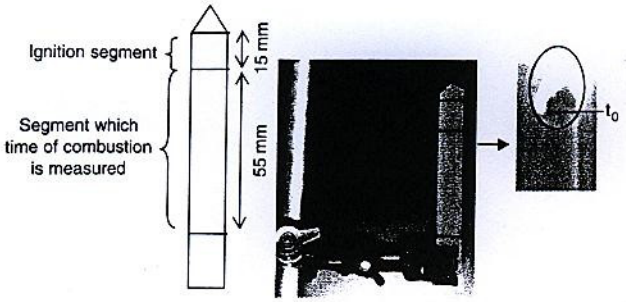

Fig. 1. Schematic representation and photograph of a nanocomposite sample for the flammability test. Time of combustion measurement was initiated (t_0) when the flame reached the second line.

the selected compatibilizer were successively added and kneaded for 7 min or 30 min (at 20 or 75 rpm).

2.3. Characterization

X-ray diffraction (XRD) was carried out by using a SIEMENS D5000 diffractometer equipped with an X-ray generator (Cu K_α radiation, $\lambda = 0.15406$ nm) at room temperature. The diffractograms were scanned in 2θ range from 1.5 to 30° at a rate of 10°/min. A transmission electron microscope (TEM), Philips CM200, was used to observe the state of dispersion of the clay stacks, using an acceleration voltage of about 120 kV on sample prepared as ultrathin section of 80 nm in thickness using an ultramicrotome Leica UCT at −130 °C. Dumbbell-shaped testing samples were cut from the molded plates and used for tensile testing at least 24 h after molding. Tensile testing was repeated for at least three samples at an extension speed of 50 mm/min with an initial distance between grips of 25.4 mm, according to the ASTM D638 V norm.

The flammability testing was performed on rectangular sections of materials cut from a molded plate where one extremity was cut into a point (Fig. 1). The upper part was set on fire with a Bunsen burner and the sample was let to burn like a candle. The time for the flame to travel from the second down to the third mark was measured. The ability of the nanocomposites to avoid the formation of burning droplets and to induce charring was also observed.

3. RESULTS AND DISCUSSION

3.1. Binary Blend of HDPE and Cloisite® 20A

A melt blend of HDPE (96 wt%) and Cloisite® 20A (4 wt%) was first prepared in order to evaluate the morphology (intercalation and state of dispersion of the nanoplatelets). Practically, HDPE pellets were pre-melted in the Brabender mixer, and then the clay was added. The recovered material was analyzed by XRD and compared with the diffractogram of the organomodified clay (Fig. 2). The basal spacing of Cloisite® 20A, which is indicated by the peak at $2\theta = 4°$ ($d = 22.6$ Å), is still present in the compounded material but slightly shifted towards

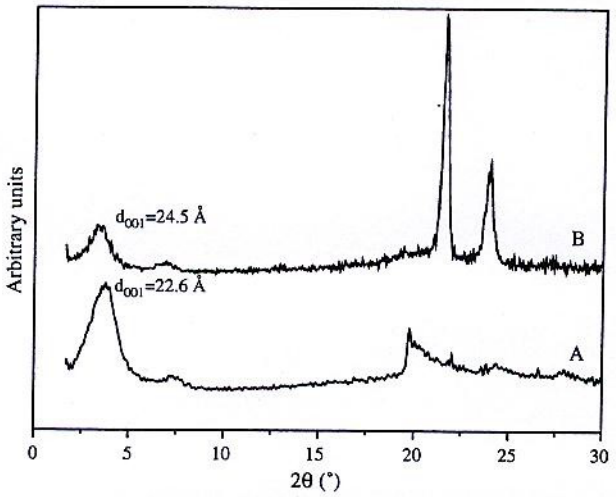

Fig. 2. X-ray diffractograms of (A) Cloisite® 20A and (B) HDPE–Cloisite® 20A compound (3 wt% in inorganics).

lower angle value with $2\theta = 3.6°$ ($d = 24.5$ Å). Secondary diffraction peak (d_{002}) is also visible near $2\theta = 7°$. The peaks at $2\theta = 21$ and 24° in the composite are related to the HDPE crystalline phase while the peak at $2\theta = 20°$ in the clay corresponds to a crystalline plane of the nanoplatelets. The increase in interlayer spacings (d_{001}) is only of 1.9 Å, such a small increase excludes any HDPE chain intercalation and is rather the consequence of clay interlayer reorganization under shear and high temperature. Thus, as expected, the so-prepared material is a (phase separated) microcomposite.

TEM observation of this microcomposite reveals (Fig. 3) large stacks of non-intercalated nanoplatelets, that appear as dark, micron-size particles while the light gray

Fig. 3. TEM micrograph of HDPE–Cloisite® 20A compound (3 wt% in inorganics). Black objects are micron-scale non-intercalated stacks of organomodified nanoplatelets.

shading that is seen is due to the crystallinity of the HDPE matrix.

3.2. Masterbatch Preparation and Characterization

Since HDPE alone is not able to intercalate in the interlayer spacing of Cloisite® 20A, one solution is therefore to take the nanolayers away from each other by increasing the interlayer spacing with intercalated polar polyolefin chains. Hence, such separated/intercalated clay platelets should be more easily dispersed within the HDPE matrix under shear. In order to promote this clay nanolayer separation, three compatibilizers, known to intercalate organomodified clays such as Cloisite® 20A and having some compatibility with HDPE have been chosen. They differ by their chemical structure and by the way they can interact with the organoclay surface. Maleic anhydride-grafted PE (MAgPE) is known to favor organoclay exfoliation when used as polymer matrix.[29,30] The maleic anhydride groups, grafted along LLDPE chains and characterized by the large dipole moment of the anhydride function, are able to strongly interact with the organoclay surface, especially with the Si–OH and Al–OH groups located at the borders of the clay platelets. However, this compatibilizer may suffer from two drawbacks: the low amount of maleic anhydride grafted along the chains (less than 1 mol%), inherent to this type of post-functionalized polyolefin and the lack of compatibility that can exist between HDPE and LLDPE. The ethylene/vinyl acetate copolymer, (EVA_{12}), with 4.25 wt% of vinyl acetate statistically scattered in the copolymer chain, is known to form partly exfoliated nanocomposites.[34–36] It interacts in a softer way with the organomodified clay, through the permanent dipole of the acetate function. As far as Kraton® (styrene-b-ethylene/butylene-b-styrene block copolymer) is concerned, literature reports the preferential interaction of the polystyrene blocks with organoclays such as Cloisite® 20A, the olefinic block being rejected outside.[37] Such organization may favor clay exfoliation when the masterbatch is dispersed in HDPE. As the HDPE has no affinity for the Cloisite® 20A, the polyolefin was not engaged in the preparation of the masterbatches. The compatibilizer (EVA_{12}, Kraton® or MAgPE) was first melted on a two-roll mill and kneaded in the presence of Cloisite® 20A (33 wt%) and the antioxidant, for 5 min. The so-formed material was recovered and transferred into the Brabender mixer in order to impose an efficient shear on the composite. XRD analysis was undertaken on the masterbatches to determine their morphological evolution (Fig. 4). The basal spacing of Cloisite® 20A, which is indicated by a peak at $2\theta = 4°$, is shifted towards lower angles: as expected, the organoclay has been intercalated by the polar chains of the selected compatibilizers. It is worth noting that the capability to increase the interlayer spacing seems to be related with the nature of the

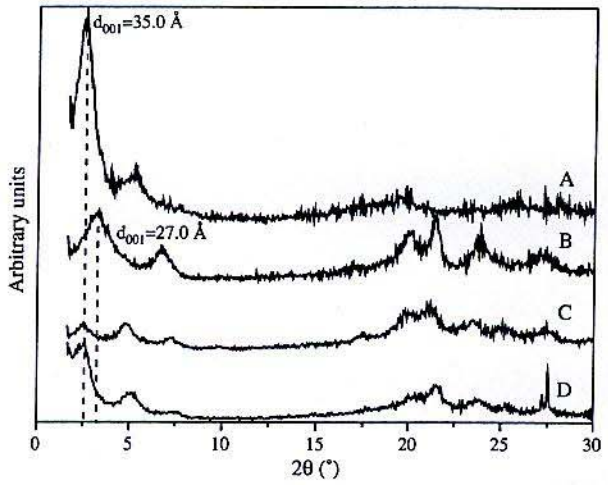

Fig. 4. X-ray diffractograms of masterbatches based on Cloisite® 20A melt blended with (A) Kraton® (33 wt% organomodified clay); (B) MAgPE (33 wt% organomodified clay); (C) EVA_{12} (33 wt% organomodified clay); (D) EVA_{12} (15 wt% organomodified clay).

polyolefin modifier. EVA_{12} and Kraton® seem to have the same tendency to intercalate as the basal peak is shifted to $2\theta = 2.5°$ $d_{001} = 35$ Å) in both cases. But the noticeable difference in peak intensity could indicate that the Kraton® copolymer preserves the ordered state of the clay. This characteristic could impede the delamination of the Cloisite® 20A. In order to check the EVA_{12} propensity to disorganize the organoclay, a fourth masterbatch-EVA_{12}-Cloisite® 20A, 85/15 wt%/wt% have been prepared wherein the filler is more "diluted." It appears that the basal peak tends to convert into a curve starting from $2\theta = 3°$ to smaller angles: this corresponds to a gradient of interlayer spacings ($d > 30$ Å). The interactions between the separated nanolayers get weaker and the state of disorder appears enhanced. Intercalation by MAgPE proved much less efficient, with the interlayer spacing increasing only from 22.6 Å to 27.0 Å. This limited extent of intercalation might result from a low degree of functionalization of the chosen MAgPE.

3.3. Preparation and Characterization of the HDPE-Based Nanocomposites

The aforementioned masterbatches were kneaded under shear with molten HDPE in order to form nanocomposites filled with 3 wt% in inorganics. They are expected to be as delaminated as possible, or at least, intercalated. Direct blending of HDPE, Cloisite® 20A and compatibilizer were also carried out for the sake of comparison. The advantage of this method is to be a fast and easy process to prepare nanocomposites. Indeed, only one blending step is required: in this case, Cloisite® 20A and the compatibilizers were successively added to the HDPE pellets, which were first pre-melted in the internal chamber in presence of the antioxidant. In each case, the residence time of the compounds in the internal chamber at 185 °C was 7 min.

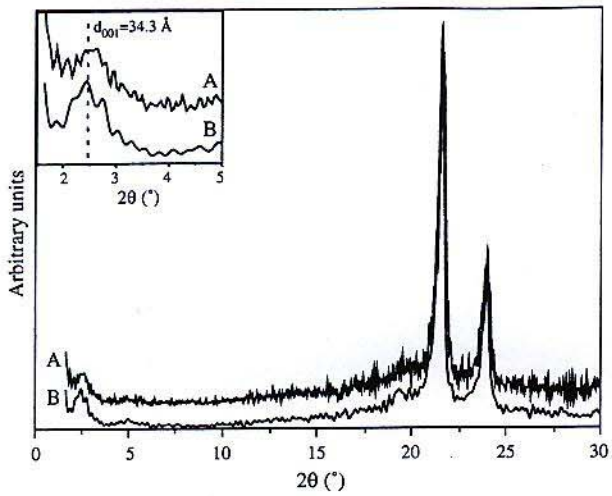

Fig. 5. X-ray diffractograms of HDPE/Cloisite® 20A nanocomposites (3 wt% in inorganics) compatibilized by 8 wt% of EVA_{12}, as produced by (A) masterbatch process (MP) and by (B) direct melt blending process (DP). Inset is a zoom of the low 2θ area of the diffractograms.

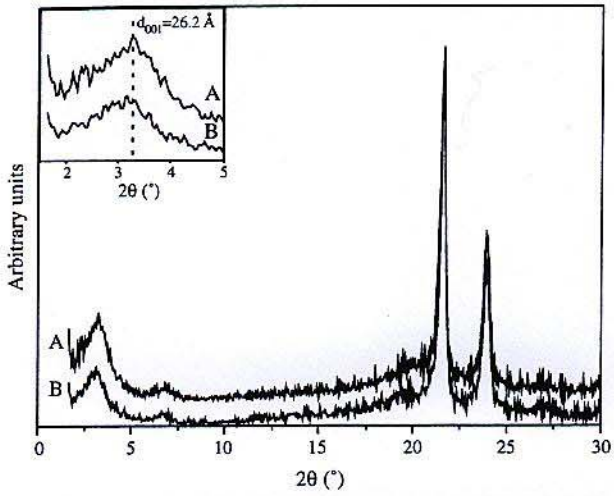

Fig. 7. X-ray diffractograms of HDPE/Cloisite® 20A nanocomposites (3 wt% in inorganics) compatibilized by 8 wt% of MAgPE, as produced by (A) masterbatch process (MP) and by (B) direct melt blending process (DP). Inset is a zoom of the low 2θ area of the diffractograms.

TEM and/or XRD analyses were undertaken and compared to each other. XRD diffractograms indicate that, whatever the compatibilizer (EVA_{12}, Fig. 5; Kraton®, Fig. 6 and MAgPE, Fig. 7) or the method of preparation, intercalated nanocomposites were essentially formed. Indeed, basal peak of intercalated Cloisite® 20A was still visible. When Cloisite® 20A was pre-intercalated with the polar copolymers in order to initiate the stacking destructuration, the layered structure of the clay remained preserved after redispersion within HDPE. On another hand, upon direct mixing of the three components, it appears that the polar copolymer selectively migrated within the clay interlayer spacings, without significantly favoring the HDPE intercalation.

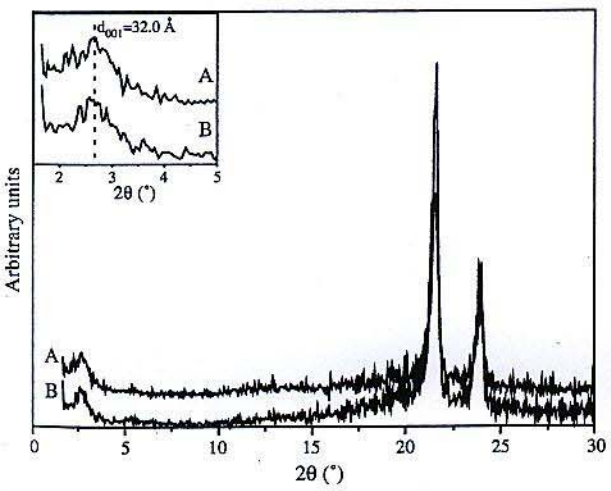

Fig. 6. X-ray diffractograms of HDPE/Cloisite® 20A nanocomposites (3 wt% in inorganics) compatibilized by 8 wt% of Kraton,® as produced by (A) masterbatch process (MP) and by (B) direct melt blending process (DP). Inset is a zoom of the low 2θ area of the diffractograms.

Although the layered structure was preserved, a part of the layers might be exfoliated. TEM analyses (Figs. 8a and b) of the nanocomposite HDPE/MAgPE/Cloisite® 20A (3 wt%, via direct melt blending process-DP) allows visualizing the actual nanoscopic structure of the material. Figure 8a shows at microscopic range that thin separated tactoids are quite homogeneously dispersed throughout the matrix. At higher magnification (Fig. 8b), tactoids made of about ten or so nanolayers can be observed. Moreover, some isolated platelets can be detected here and there (see arrows). These micrographs indicate that a form of delamination has occurred during the melt compounding process, which reduces the size of the tactoids and even delivers some individually spread nanoplatelets, even if the compatibilizer is bearing a low amount of polar groups (less than 1 mol%) and if LLDPE is rather incompatible with the HDPE matrix.

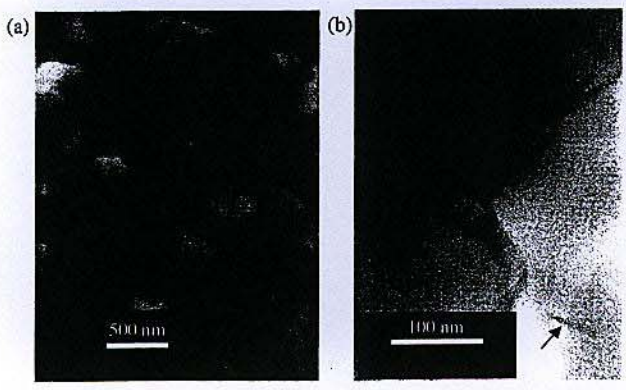

Fig. 8. TEM micrographs of the HDPE/Cloisite® 20A nanocomposite (3 wt% in inorganics) compatibilized by 8 wt% of MAgPE by direct melt blending process (DP) (a) at low resolution; (b) at high resolution (arrows indicate individual clay nanoplatelets).

RESEARCH ARTICLE

3.4. Effect of Shear Force and Blending Residence Time on Morphology of Cloisite® 20A

A longer kneading (30 min) might favor the exfoliation. In order to check it, two nanocomposites have been prepared by direct melt blending in the internal chamber with a residence time of 30 min, instead of 7 min as first studied. Difference in shear rate has been accordingly investigated, first at low shear rate (at 20 rpm), then at higher rate (75 rpm). Given that EVA_{12} has triggered the larger increase of the interlayer spacing, this copolymer was chosen as compatibilizer, since it appeared to be more susceptible to reach the exfoliation state more readily. The recovered materials were analyzed by XRD and TEM to determine their morphology. The diffractograms (Fig. 9) of both nanocomposites show an intense basal peak located at $2\theta = 2.6°$ ($d = 34$ Å): this indicates the presence of intercalated and probably well-ordered stacks of nanolayers. Longer kneading time thus seems to limit additional delamination of the organoclay in the HDPE matrix, whatever the shear rate. This analysis is confirmed by TEM observations where thin and isolated tactoids are observed (Figs. 10a and b).

3.5. Mechanical Properties of the (Nano)Composites: Tensile Tests

As aforementioned, the melt blends of HDPE and Cloisite® 20A in presence of the studied functionalized PE generated essentially intercalated nanocomposites. It has been established by TEM analysis that the recovered materials are made of thin tactoids that are dispersed throughout the matrix. This morphology, intermediate to a true delaminated one, might be able to strengthen the HDPE matrix. Tensile properties of the nanocomposites have been

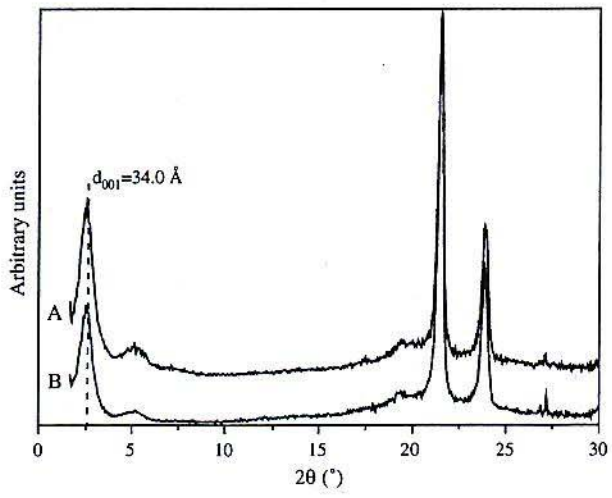

Fig. 9. X-ray diffractograms of HDPE/Cloisite® 20A nanocomposites (3 wt% in inorganics) compatibilized by 8 wt% of EVA_{12}, as produced by direct melt blending process (DP) during 30 min at (A) 75 rpm and (B) 20 rpm.

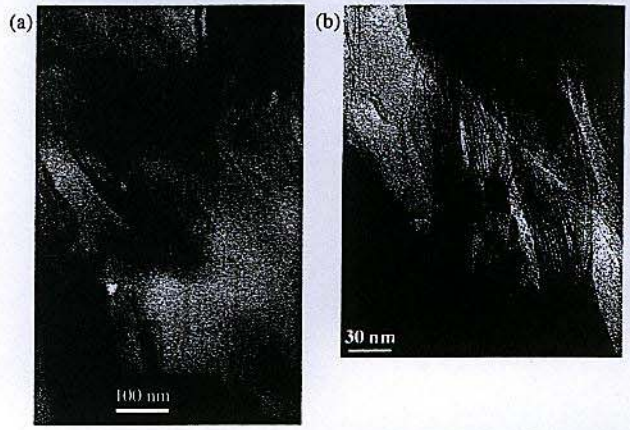

Fig. 10. TEM micrographs of the HDPE/Cloisite® 20A nanocomposite (3 wt% in inorganics) compatibilized by 8 wt% of EVA_{12} by direct melt blending process (DP) during 20 min at (a) 75 rpm; (b) 20 rpm.

investigated and compared with both the unloaded HDPE matrix and its simple blends with each of the investigated compatibilizers, but also the HDPE–Cloisite® 20A microcomposite (Table I). It appears that the fact of introducing a polar compatibilizer (8 wt%) in the HDPE matrix leads to a notable loss of the Young modulus and an increase in the strain at break (compare samples 1, 3, 8, and 11 in Table I): this can be explained by a limited miscibility between the HDPE and the compatibilizers and/or by a plasticizer effect of the compatibilizer.

For the EVA_{12} compatibilizer, a significant increase in Young's modulus is observed, especially for the samples prepared by the masterbatch process, however at the detriment of the ultimate properties (compare entries 3 and 6). Increasing the blending time from 7 min (entry 6) to 30 min (entry 7) tends to improve slightly the strain at break. In contrast, direct melt blending (entry 4) is characterized by a lower improvement in stiffness (small increase in Young's modulus) and low shear rate, even for a long residence time (entry 5) does not improve the stiffness at all.

As far as the Kraton® compatibilizer is concerned, the nanocomposite preparation either by the masterbatch process or the direct melt blending process does not improve the tensile properties. These intercalated nanocomposites behave very much like microcomposites (compare entries 8, 9, and 10). Finally, the MAgPE compatibilizer is characterized by a small improvement in the Young's modulus when used with the masterbatch process (compare entries 11 and 13) but no significant improvement in stiffness can be found for the nanocomposite prepared by the direct melt blending (entry 12) even for longer blending time (entry 14). This might reflect the incompatibility between the HDPE matrix and the LLDPE-based compatibilizer that limits interactions of the latter with Cloisite® 20A during direct melt blending, while in case of the masterbatch, the MA-g-PE is directly in contact with the clay and intercalate it.

Table I. Tensile properties of the HPDE matrices, it blends with each of the studied compatibilizers and related (nano)composites in function of melt processing (DP or MP) and extent of shear rate. Compatibilizer content: 8 wt%; compounding time 7 min.

Entry	Compatibilizer	Filler content (wt%)	Process	Shear rate (rpm)	Young's modulus (MPa)	Strain at break (%)
1	None	0	DP	75	499±39	310±86
2		3	DP	75	485±35	525±41
3	EVA_{12}	0	DP	75	466±7	828±23
4		3	DP	75	517±42	293±72
5		3	DP	20[a]	441±52	632±68
6		3	MP	75	618±92	110±102
7		3	MP	75[a]	582±39	235±172
8	Kraton®	0	DP	75	448±26	743±81
9		3	DP	75	448±26	310±234
10		3	MP	75	356±24	525±98
11	MAgPE	0	DP	75	432±8	843±432
12		3	DP	75	448±27	364±103
13		3	MP	75	480±28	303±96
14		3	DP	20[a]	451±4	501±56

[a]Compounding time: 30 min.
DP = one-step melt blending process.
MP = two-step masterbatch process.

In term of stiffness improvement, the best compatibilizer is therefore EVA_{12} especially when involved in the masterbatch process. To improve properties at break, longer blending times are recommended. Under these conditions, reinforcement is insured by thin stacks of intercalated nanoplatelets (together with some individually spread nanoplatelets).

3.6. Flame Behavior of the Nanocomposites

In order to investigate the flame behavior of the prepared nanocomposites, an indicative fire test has been designed (see experimental details). Time of combustion for different HDPE-based nanocomposites are given in Table II.

The HDPE/Cloisite® 20A microcomposite (3 wt% in inorganics, entry 2) shows already a noticeable fire retarding effect when compared to a reference microcomposite based on a 3 wt% dispersion of natural (non-organomodified) clay in the same HDPE matrix (entry 1): the time of combustion is longer and carbonaceous residues are visibly formed. This could indicate that, although HDPE and the nanofiller are poorly compatible chemically, organoclay stacks were sufficiently dispersed in the HDPE matrix to induce some effect on the flammability behavior. Comparing the result obtained for materials including the EVA_{12} compatibilizer (entries 3 to 6), the best results are obtained for the nanocomposite prepared under high shear rate and for a long blending time. As far as the MAgPE compatibilizer is concerned (entries 7 and 8), the resulting essentially intercalated nanocomposite seems to be also very efficient for increasing the combustion time of the material. Furthermore, when observing the burning behavior (Fig. 11), the nanocomposite materials are characterized by a drastic diminution of burning droplet formation (very limited dripping effect) and a modification of the combustion behavior, where a significant charring appears for (at least) intercalated nanocomposites.

Table II. Combustion time for various (nano)composites prepared by the direct melt blending process using 8 wt% of EVA_{12} or MAgPE as compatibilizer. Effect of processing conditions.

Entry	compatibilizer	Filler content (wt%)	Blending time (min)	Shear rate (rpm)	Combustion time (sec)
1	—	3[a]	7	75	70
2	—	3	7	75	324
3	EVA_{12}	0	7	75	102
4	EVA_{12}	3	7	75	340
5	EVA_{12}	3	30	75	475
6	EVA_{12}	3	30	20	351
7	MAgPE	0	7	75	90
8	MAgPE	3	7	75	415

[a]3 wt% of a natural montmorillonite (Cloisite® Na) was used for the sake of comparison.

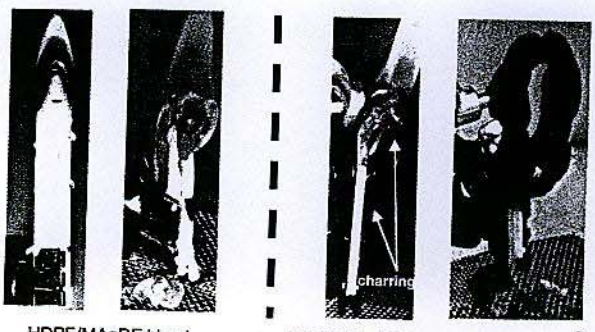

Fig. 11. Burning behavior of a HDPE/MAgPE blend and its 3 wt% Cloisite® 20A nanocomposite counterpart.

4. CONCLUSIONS

The efficiency of EVA_{12}, Kraton® and MAgPE as compatibilizers for the formation of HDPE/clay nanocomposites has been investigated. While no true and complete delamination can be obtained using these compatibilizers, significant differences in terms of morphologies and properties have been observed, depending on both the type of compatibilizer and the process conditions used to prepare the nanocomposite. As far as the compatibilizer nature is concerned, EVA_{12} appears to be the one that allows obtaining the best thin nanoplatelets stacks dispersion. This dispersion induces a significant increase in the Young's modulus of the resulting nanocomposite and an enhanced flame resistance. Neither MAgPE nor Kraton® was able to promote such an improvement in morphology and properties. With the strong dipole moment of the cyclic anhydride moieties pending along the polyolefinic chains, MAgPE might be interacting too strongly with the clay borders (via the Si–OH and Al–OH bonds), limiting clay exfoliation. Furthermore, the lack of compatibility between LLDPE and HDPE may be a supplementary cause for the low amount of exfoliation observed in the resulting melt blends. As far as Kraton® is concerned, intercalation within the organomodified clay seems to be extremely stable, precluding any nanoplatelets delamination.

Processing conditions are also important in improving morphologies and properties. Best stack delamination has been observed for nanocomposites prepared using a two-step process via the preparation of a compatibilizer/organomodified clay masterbatch, followed by its dispersion in the HDPE matrix. Moreover, high shear rate and long blending time proved to improve the dispersion of the thin nanoplatelet stacks and hence the overall mechanical and fire properties of the resulting nanocomposites.

Acknowledgments: M. M. is much indebted to Total Petrochemical Research Feluy for financial support in the frame of his Ph.D grant. The authors are very grateful for the financial support from "Région Wallonne" and European Community (FEDER, FSE) in the frame of "Pôle d'Excellence Materia Nova." LMPC thanks the Belgian Federal Government Office of Science Policy (STC-PAI 5/3).

References and Notes

1. M. Alexandre and Ph. Dubois, *Mater. Sci. Eng. R* 28, 1 (**2000**).
2. M. Biswas and S. S. Ray, *Adv. Polym. Sci.* 155, 167 (**2001**).
3. D. Schmidt, D. Shah, and E. P. Giannelis, *Curr. Opin. Solid State Mater. Sci.* 6, 205 (**2002**).
4. F. Gao, e-Polymer n°004 (**2002**).
5. A. Okada, M. Kawasumi, A. Usuki, Y. Kojima, T. Kurauchi, and O. Kamigaito, *Mater. Res. Soc. Proc.* 171, 45 (**1990**).
6. C. Zilg, F. Dietsche, H. Botho, C. Dietrich, and R. Mulhaupt, *Macromol. Symp.* 169, 65 (**2001**).
7. T. Srikhirin, A. Moet, and J. B. Lando, *Polym. Adv. Technol.* 9, 491 (**1998**).
8. Y. Kojima, K. Fukumori, A. Usuki, A. Okada, and T. Kurauchi, *J. Mat. Sci. Lett.* 12, 889 (**1993**).
9. H. Lu, Y. Hu, Q. Kong, Y. Cai, Z. Chen, and W. Fan, *Polym. Adv. Technol.* 15, 601 (**2004**).
10. J. W. Cho and D. R. Paul, *Polymer* 42, 1083 (**2001**).
11. L. M. Liu, Z. N. Qi, and X. G. Zhu, *J. Appl. Polym. Sci.* 71, 1133 (**1999**).
12. Y. Kojima, A. Usuki, M. Kawasumi, A. Okada, T. Kurauchi, and O. Kamigaito, *J. Appl. Polym. Sci.* 49, 1259 (**1993**).
13. K. Yano, A. Usuki, and M. Kawasumi, *J. Appl. Polym. Sci.* 49, 1259 (**1993**).
14. R. A. Vaia, H. Ishii, and E. P. Giannelis, *Chem. Mater.* 5, 1694 (**1993**).
15. R. A. Vaia and E. P. Giannelis, *Macromolecules* 30, 8000 (**1997**).
16. J. T. Yoon, W. H. Jo, M. S. Lee, and M. B. Ko, *Polymer* 42, 329 (**2001**).
17. S. S. Ray, P. Maiti, M. Okamoto, K. Yamada, and K. Ueda, *Macromolecules* 35, 3104 (**2002**).
18. E. Manias, A. Touny, L. Wu, K. Strawhecker, B. Lu, and T. C. Chung, *Chem. Mater.* 13, 3516 (**2001**).
19. N. Furuichi, Y. Kurokawa, K. Fulita, A. Oya, H. Yasuda, and M. Kiso, *J. Mater. Sci.* 31, 4307 (**1996**).
20. H. G. Jeon, H. T. Jung, S. W. Lee, and S. D. Hudson, *Polym. Bull.* 41, 107 (**1998**).
21. C. B. Liu, T. Tang, Z. F. Zhao, and B. T. Huang, *J. Polym. Sci. Part A* 40, 1892 (**2002**).
22. J. C. Lin, L. C. Hwu, L. C. Chou, C. H. Chan, and Q. J. Jiang, *Polym. Prep.* 45, 874 (**2004**).
23. Q. Wang, Z. Zhou, L. Song, H. Xu, and L. Wang, *J. Polym. Sci. Part A* 42, 38 (**2004**).
24. J. Heinemann, P. Reichert, R. Thomann, and R. Mulhaupt, *Macromol. Rapid Commun.* 20, 423 (**1999**).
25. S. Duquesne, C. Jama, M. Le Bras, R. Delobel, P. Recourt, and J. M. Gloaguen, *Comp. Sci. Technol.* 63, 1141 (**2003**).
26. M. Alexandre, G. Beyer, C. Henrist, R. Cloots, A. Rulmont, R. Jérôme, and Ph. Dubois, *Macromol. Rapid Commun.* 22, 643 (**2001**).
27. M. Zanetti and L. Costa, *Polymer* 45, 4367 (**2004**).
28. T. H. Chuang, W. Guo, K. C. Cheng, S. W. Chen, H. T. Wang, and Y. Y. Yen, *J. Polym. Res. Taiwan* 11, 169 (**2004**).
29. K. H. Wang, M. H. Choi, C. M. Koo, Y. S. Choi, and I. J. Chung, *Polymer* 42, 9819 (**2001**).
30. C. M. Koo, H. T. Ham, S. O. Kim, K. H. Wang, and I. J. Chung, *Macromolecules* 35, 5116 (**2002**).
31. T. G. Gopakumar, J. A. Lee, M. Kontopoulou, and J. S. Parent, *Polymer* 43, 5483 (**2002**).
32. J. Zhang and C. A. Wilkie, *Polym. Deg. Stab.* 80, 163 (**2003**).
33. H. R. Dennis, D. L. Hunter, D. Chang, S. Kim, J. L. White, J. W. Cho, and D. R. Paul, *Polymer* 42, 9513 (**2001**).
34. F. Zhang and U. Sundararaj, *Polym. Comp.* 25, 535 (**2004**).
35. I. S. Suh, D. H. Ryu, J. H. Bae, and Y. W. Chang, *J. Appl. Polym. Sci.* 94,1057 (**2004**).
36. C. H. Jeon, S. H. Ryu, and Y. W. Chang, *Polym. Int.* 52, 153 (**2003**).
37. A. S. Silva, C. A. Mitchell, M. F. Tse, H. C. Wang, and R. Krishnamoorti, *J. Chem. Phys.* 115, 7166 (**2001**).

Received: 26 March 2005. Revised/Accepted: 8 June 2005.